Progress in testing exo-planet signal extraction on the TPF-I Planet Detection Testbed

Stefan R. Martin, Piotr Szwaykowski, Frank M. Loya, Kurt Liewer
Jet Propulsion Laboratory, California Institute of Technology, Pasadena, CA
Email: Stefan.R.Martin@jpl.nasa.gov

ABSTRACT

The TPF Interferometer (TPF-I) concept is being studied at the Jet Propulsion Laboratory and the TPF-I Planet Detection Testbed has been developed to simulate the detection process for an earthlike planet orbiting a star within about 15 pc. The testbed combines four beams of infrared light simulating the operation of a dual chopped Bracewell interferometer observing a star and a faint planet. This paper describes the results obtained this year including nulling of the starlight on four input beams at contrast ratios up to 250,000 to 1, and detection of faint planet signals at contrast ratios with the star of 2 million to 1.

Keywords: Nulling, Stellar Interferometry, Exoplanet

1. INTRODUCTION

In the last decade or so the radial velocity technique has been successfully employed to detect many planets in orbit around other stars. The technique, which relies on sensitive measurements of the Doppler shift of spectral absorption features, is most sensitive to massive planets in the orbiting close to the star. The Terrestrial Planet Finder (TPF) project seeks to add new types of extrasolar planets to the known set by detecting small rocky planets similar to the innermost planets of our solar system. Such planets should be detectable using interferometry or advanced coronagraphy with the high optical stability available on space platforms and the TPF project has been studying both mission concepts. A coronagraph would operate near the visible wavelength range (about 0.6 to 1.0 micron) and an interferometer would operate in the near infrared between about 7 and 17 micron. The data from such systems would enable characterization of exoplanet atmospheres and detection of gases associated with life, for example, oxygen has spectral features in the coronagraph waveband and carbon dioxide has prominent features in the interferometer waveband[1]. The two mission concepts are markedly different in form: the coronagraph would employ a single large telescope, while the interferometer studied at JPL would utilize four free flying telescopes with a fifth beam combiner spacecraft. However, the systems share a single basic concept, that is some method of drastically reducing the flux of light from the star and thus enabling direct optical detection of a planetary system in orbit, which is normally impossible because of the glare from the star. To be successful in the detection of earth-like planets at visible wavelengths, the starlight must be reduced by a factor of approximately 10^9. Owing to the improved star:planet contrast ratio in the near infrared compared to the visible, an interferometer must be capable of reducing the starlight in the science beam train by a lesser factor of approximately 10^6. The coronagraph performs the reduction of starlight using entrance pupil apertures and focal plane masks and a sophisticated wavefront correction system to physically block the starlight[2]. The interferometer uses the technique of nulling interferometry[3] to separate the starlight from the planet light.

At the Jet Propulsion Laboratory (JPL) a number of testbeds have been built to support technical goals for planet detection using both technologies. The most prominent testbeds are: on the coronagraph side, the High Contrast Imaging Testbed, and on the interferometer side, the nulling testbeds (Planet Detection, and Achromatic Nulling) and formation flying testbed (Formation Control Testbed). Contrast ratios of the necessary magnitudes have been demonstrated on JPL testbeds for both the interferometer and the coronagraph and so these major technical performance requirements are within reach. On the nulling technology side, the work has been divided principally between a smaller testbed intended to show deep nulling over a broad band, and a larger testbed using laser nulling, but intended to show highly stable, deep nulling performance and faint planet signal detection. In addition, up till recently, JPL together with

other institutions performed design work that mapped out engineering designs for the interferometer and the coronagraph.

This paper concerns the recent performance and operation of JPL's Planet Detection Testbed, which emulates the operation of the interferometric beam combiner. For successful operation in space the interferometer will need to achieve deep nulls of order one million to one, enabling detection of planets almost three times fainter, corresponding to earthlike planets seen from 15 pc. Deep nulling performance is effectively a requirement for symmetry; the two incoming beams that are combined must have near identical properties. To null the starlight, two apertures collect identical fluxes of light from the star. One of the incoming beams is inverted in phase by addition of an achromatic π phase shift, and when the two beams are interferometrically combined, the starlight is destructively interfered. Any imbalance between the beams in terms of flux would leave some residual light in the output, and a number of other effects such as phase and polarization differences also produce residual light[4]. To achieve deep nulls, these small residual effects must be controlled. From a larger perspective, to achieve planet detection, two nulling performance goals have to be maintained. The first goal is broadband, deep nulling. Under the JPL design concept, the passband would be divided into two, so that two sets of nullers would be used in tandem, one working in the 7 to 11 μm band, and the other in the 11 to 17 μm band. The reason for splitting the band into two is primarily to facilitate design of coatings for the beamtrain optics and allow the use of single mode fibers in the detection stage. Such coatings and fibers have reasonably wide, but ultimately limited bandwidths, necessitating passband division. In the future, it is possible that improved beamcombiner concepts might be developed that would simplify the system down to a single set of optics. Broadband nulling implies good intensity balance across the band; it also implies an overall optical phase difference between the beams very near to π across the band. Achieving the desired level of symmetry across the passband implies control of the null at one moment in time. In JPL's concept, the optical beamtrain would include a device called the Adaptive Nuller (also a JPL testbed) which allows small chromatic asymmetries in optical path and amplitude in the four beam trains to be corrected. This device operates on the temporally static differences which arise for example from small coating or mirror surface differences.

The second nulling goal is maintenance of the null during the period of observation, proofing it against changes in the alignment or phasing of the optical system. These changes are an interesting aspect of the observational process; and can be divided two timescales. The shorter timescales correspond to rapid processes, for example vibration of the telescopes caused by reaction wheel forces, say from one to one hundredth of a second. Longer timescales could be characterized as drifting processes, for example as the telescopes move slowly in space relative to one another. These slower processes are of particular concern since observations of a planetary system will typically take 10 hours, involving a single rotation of the telescope array around the line of sight to the star. If one of the incoming starlight beams is allowed to drift off the detector, nulling performance will be degraded and starlight will leak through the system. This leakage light is difficult to distinguish from planet light and the slow variation in this leakage will become confused with the slowly varying planet signal. Therefore the interferometer will be equipped with alignment systems which monitor and control the incoming beams. The sensors that provide the signals for the alignment are also subject to drifting, and will typically exhibit more drift at longer periods, necessitating occasional recalibration. Since the slow drifts are at timescales similar to those of the planet signal itself, good alignment and phase control over long timescales becomes a *sine qua non* for planet detection. The two principal JPL nulling testbeds are intended to cover these two performance goals. The ANT covers goal one, broadband nulling, and the PDT covers goal two, stable nulling. As part of this stable

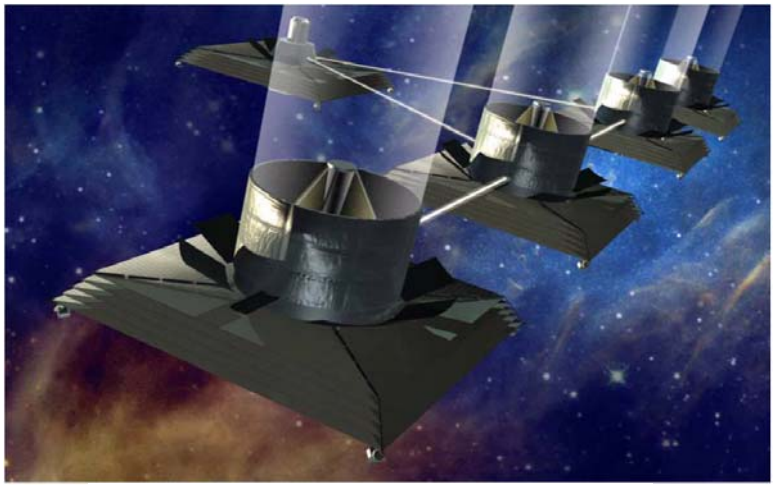

Figure 1: Linear array of four space telescopes.

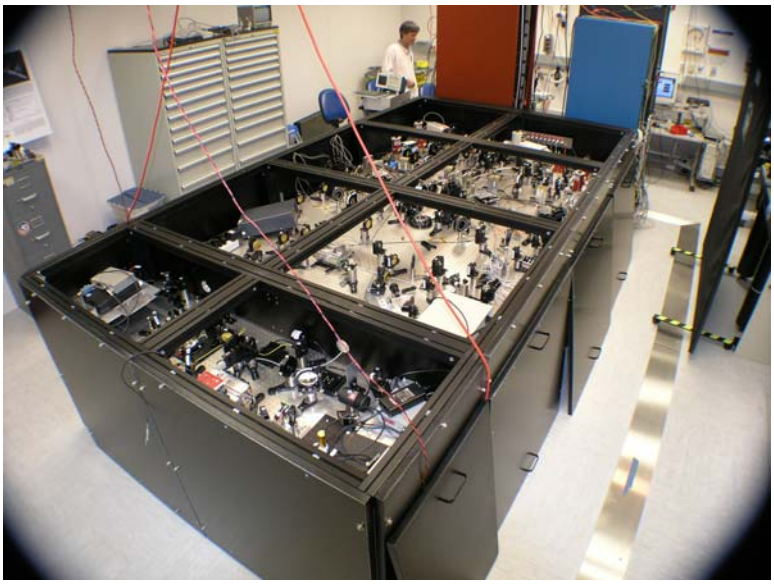

Figure 2: The TPF-I Planet Detection Testbed

nulling goal, PDT simulates an entire observation process including formation rotation.

One possible TPF telescope formation is illustrated in figure 1. In this system, four telescopes with 4 m diameter apertures are arrayed in a line with a fifth spacecraft supporting the beamcombiner positioned nearby. A number of array configurations have been and are being considered[5], for example, five and six spacecraft two-dimensional arrays have been studied, three and four spacecraft linear and 2D arrays and also more recently, arrays with the beamcombiner spacecraft out of plane with respect to the collector telescopes. Current modeling at JPL favors a rectangular in-plane array of four telescopes with roughly 3:1 aspect ratio and a central beamcombiner spacecraft. The PDT (figure 2) is set up as a four beam testbed, and is capable of simulating rectangular or linear four-telescope arrays; it is currently set up as a linear array.

A single pair of telescopes produces a simple interference pattern on the sky. The array is phased on the star with a π phase inversion in one arm, and the star is then located in a dark or null fringe, substantially reducing its apparent flux. The spacing of the interference fringes on the sky is determined by the array spacing and would be set up before the observation, taking into account the angular diameter of the star and the angular distance to the habitable zone in which targets of the greatest interest might be observed. ?? If a planet exists near the star, it would be most detectable if it appeared on the bright fringe adjacent to the central null. Having nulled the star, an appreciable background of ~1000 photon/s would remain. This background comes primarily from three sources: local zodiacal light from dust in our own solar system, exo-zodiacal light from dust in the system being observed, and null leakage light from imperfections in the nulling setup and from the finite width of the null fringe compared to the stellar diameter. The planet would produce a signal of approximately 1 photon/s so, to distinguish it from the background, the planet light will be modulated at a fixed frequency allowing a synchronous detection process to be used. To enable this detection a phased array is set up with a second pair of telescopes also nulling the starlight. By modulating the phase between the two sets of telescopes, the planet light can be alternately constructively and destructively interfered, revealing it against the background. There is one more major component of the observation process, that is rotation of the array around the line of sight to the star. This allows the fringes to be swept across the whole sky, enabling the detection of planets in almost the entire field of view.

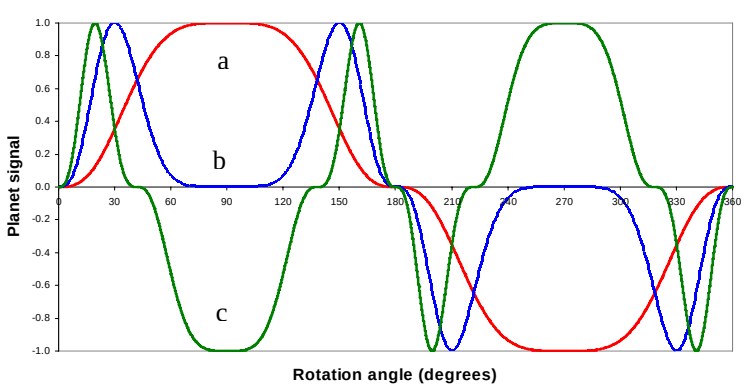

Figure 3: Signals from individual planets at three distances from the star; a) on the first constructive fringe, b) twice as far away, c) three times as far away.

Taking the case of a single planet positioned near the star, the signal from the 4-telescope linear array would have the form shown by the lines in Figure 3 where each line corresponds to different angular separations from the star. The signals vary relatively slowly as the array rotates so that the signatures could be concealed if the null depth varied similarly slowly owing to alignment and phasing drifts. While the local

zodiacal light would be expected to be a more or less constant background, and the exo-zodiacal light might have some structure corresponding to an uneven distribution of dust in the observed system, the null itself and the associated stellar leakage is a function of the observing instrument and will vary at all timescales, affecting the ability to resolve any planets. The precise way in which the null varies with small changes in light intensity and phase has been investigated theoretically in some depth[6] and a prominent effect is the cross-coupling of small electric field amplitude and phase errors across the array which produces signals that are not removed by the planet modulation process. The amplitude-phase cross-coupling will also arise in the PDT (but not the related stellar leakage term) and so can be tested against the model, and the ability to control it can also be demonstrated.

2. Modeling fluctuations in the null

A simple model analogous to the PDT was built by assuming that the statistical variability of the measured beam intensity and of the relative optical phase both follow a 1/f spectrum. Therefore the fluctuations rise in amplitude with increasing timescale, an effect commonly observed in physical systems. The photon flux from the star (or laser source) produces an intensity I_i in each beam of the 4-beam system which varies with time. Taking the complex electric field amplitude in the ith beam to be A_i, and its phase to be ϕ_i, then the instantaneous amplitude of the starlight is S_i:

$$S_i = A_i \cos(\phi_i) + j\, A_i \sin(\phi_i) \tag{1}$$

Applying the π phase shift to one beam, and combining the light from telescopes 1 and 3 numbered along the linear array, the output of one nuller is given by

$$S_{12} = A_1 \cos(\phi_1) + A_3 \cos(\phi_2+\pi) + j\, [A_1 \sin(\phi_1) + A_3 \sin(\phi_2+\pi)] \tag{2}$$

And a similarly for the second nuller using telescopes 2 and 4. A similar analysis to the following can be written for the rectangular array.

Applying the phase chop to the combined nuller outputs the output of one side of the cross-combiner is:

$$\begin{aligned} S_{1234} = {} & A_1 \cos(\phi_1) + A_3 \cos(\phi_2+\pi) + A_2 \cos(\phi_2\pm\pi/2) + A_4 \cos(\phi_4+\pi\pm\pi/2) \\ & \pm j\, [A_1 \sin(\phi_1) + A_3 \sin(\phi_3+\pi) + A_2 \sin(\phi_2\pm\pi/2) + A_4 \sin(\phi_4+\pi\pm\pi/2)] \end{aligned} \tag{3}$$

Since the planet has a small angular offset ω from the line of sight to the star, its phase has a slope across the apertures so that the phase at the ith aperture can be modeled by:

$$\psi_i = (2i - 5) \cos(\theta)\, \pi\, R\, \omega / \lambda \tag{4}$$

where θ is the angle between the line joining the star to the planet and the line forming the linear array with inter-telescope spacing R. This simple expression for the phase seen at one telescope produces the complex patterns observed in figure 3. Since the planet signal is much weaker than the star, the amplitude and phase fluctuations introduced by the beam train can be neglected so that the planet signal amplitude is:

$$\begin{aligned} P_{1234} = {} & \alpha_1 \cos(\psi_1) + \alpha_3 \cos(\pi+\psi_3) + \alpha_2 \cos(\psi_2\pm\pi/2) + \alpha_4 \cos(\pi+\psi_4\pm\pi/2) \\ & \pm j\, [\alpha_1 \sin(\psi_1) + \alpha_3 \sin(\psi_3+\pi) + \alpha_2 \sin(\psi_2\pm\pi/2) + \alpha_4 \sin(\psi_4+\pi\pm\pi/2)] \end{aligned} \tag{5}$$

where α_i is the amplitude from one telescope. When the planet is located in the first constructive fringe, $\omega = \lambda / 2R$, $\psi_1 = -\pi/2$ and $\psi_3 = 3\pi/2$ so that the phase difference between beams 1 and three has the value 2π, producing constructive interference of the planet light. Similarly there is a phase difference of 2π between beams 2 and 4. Beam 2 has phases $\pm\pi/2$ so that between sets of beams 1,3 and 2,4, the chop of $\pm\pi/2$ produces alternate constructive and destructive interference of the planet light.

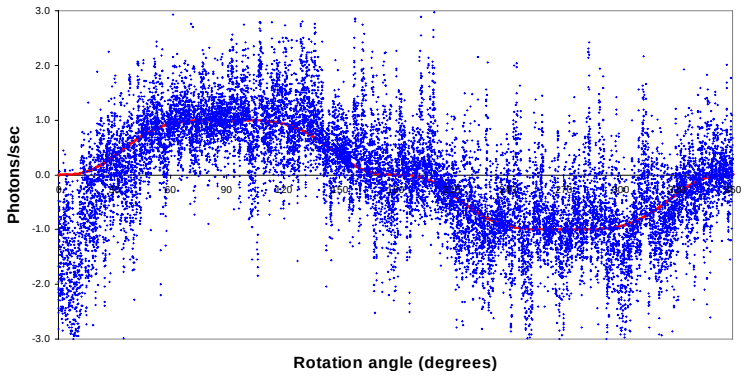

Figure 4: Variation of planet signal as the array rotates (line), and scatter plot showing the effect of disturbances to the null.

By building these expressions into a suitable model it can be shown by testing that small amplitude imbalances between the input beams to one nuller are removed by the chopping, and similarly, phase imbalances between those are also removed. However, across the array, an amplitude together with a phase deviation from the nominal values between the nullers will produce an output signal that is not removed by the chop. By a Monte Carlo simulation it can be shown that the rms phase and amplitude errors allowed in each beam are approximately 1.7 nm and 0.1%. Figure 4 shows a simulation of the planet signal during a complete rotation of the array. The planet is 1 million times fainter than the star. The blue dots show the signal with null disturbances added. This planet signal is readily detectable, having a signal to noise ratio (SNR) of ~17, and even fainter planets are also detectable because the forms of the signals are known and the output can be tested for every possible planet location. The rms phase and amplitude errors quoted allow planets 3 million times fainter than the star to be detected at an SNR of 5. This simple model was found to be in good agreement with the full model[6]. The modeling process can be used to illustrate the random disturbances to the null which occur on all timescales and mix to produce signals similar to those of planets. One important role of the PDT in the TPF testbed suite is therefore to show that the time component of the nulling task can be controlled to a level enabling the detection and ultimately the spectroscopy of target planets.

3. Planet Detection Testbed

3.1. Layout

The testbed layout has been described elsewhere[7] and so will not be detailed here; an artificial star is formed from the output of a CO_2 laser and a small thermal source. The CO_2 laser light is the 10 μm radiation which is to be nulled and the thermal source provides 2 to 4 μm radiation which is used for fringe tracking on the star. The starlight is passed through a pinhole and chopper and then split into two beams. These beams are split again forming four beams and, at this second splitting stage, simultaneously combined with beams from a second thermal source. This second source, band-limited to radiation between 10 and 11 μm, forms the artificial planet. The phase between the planet and the star is fixed so that the planet is always constructively interfered when the starlight is nulled. The planet light has a separate chopper, which can be either synchronized with the starlight chopper or run independently.

Next, the four star and planet beams enter the section of the testbed corresponding to the beamcombiner. The four beams are recombined in pairs on the nulling beamsplitters where the starlight is directed to the “star side” of the system (figure 5) and the planet light from the two nullers (directed to the “planet side”) is combined at the nulling cross-combiner beamsplitter. A second cross-combiner beamsplitter is also located on the star-side of the output (for clarity this is not shown). At the planet-side cross-combiner, the planet signal will ultimately be detected by phase chopping or more accurately optical path chopping across the telescope array. In the experiments to be described here, the planet was detected by other means. Having been combined at the cross-combiner beamsplitter the light was directed to a parabolic mirror and focused onto a small pinhole, below one wavelength in diameter. This pinhole, 8 μm in diameter and 12 μm thick, served as a single mode spatial filter. The single mode filter is a valuable part of the detection process since it reduces the sensitivity of the null to misalignments and wavefront errors. (Part of the TPF-I development is aimed at production of single mode near-infrared fibers, and two experimental types have been developed and are being used in current testbed experiments.) The infrared light was collected from the output of the fiber and focused onto a HgCdTe detector.

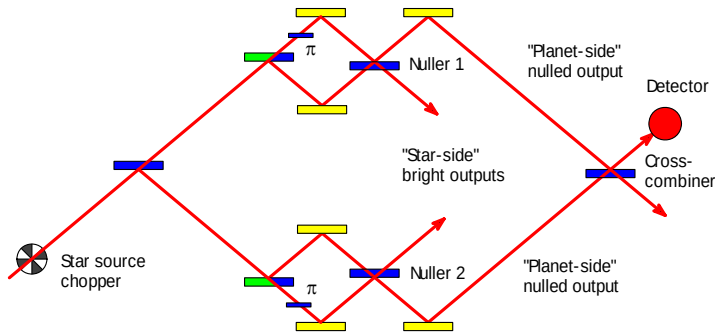

Figure 5: Layout of testbed for 4-beam nulling experiment.

The fringe tracking system consists of pairs of InSb detectors arranged on either side of each beamsplitter. Since a pair of detectors is used, the fringe trackers can be made insensitive to any fluctuations of the light source intensity. It can be shown that, if the ratio of reflected to transmitted light at the beamsplitter is M at the fringe tracking wavelength, then the phase is given by the expression $\cos \phi = (I_A (M + 1/M)/2 - I_B) / (I_A + I_B)$ where I_A and I_B are the measured intensities on either side of the beamsplitter. Thus since I_A and I_B are derived from the same source, then the expression is invariant with respect to source intensity. It is however, modified by the local fringe visibility or by beam alignment errors. Both nullers have a pair of fringe tracking detectors, and both cross-combiners have a pair, enabling tracking across the formation on either start-side or planet-side light. This arrangement allows for various phasing and wavelength options for the fringe trackers[10] leading to different testbed control possibilities.

The second part of the fringe tracking system is the metrology system. Twelve laser metrology gauges are used to monitor the optical paths on the four beams. Four gauges measure back to the source beamsplitter, four measure forward to the planet-side cross-combiner beamsplitter, and four to the star-side cross-combiner beamsplitter. The laser metrology system is used to maintain phase for high speed disturbances that cannot be tracked on the fringe trackers owing to their relatively low signal to noise ratio. Such disturbances might be caused by ambient environmental noise. In this layout, the metrology system follows the flight design concept[8] with the exception that it has source metrology. So, to remain faithful to the fundamental physics, the source side metrology gauges outputs are high pass filtered (in software) so that only the fringe trackers provide phasing information on the star.

3.2. Testbed control system

The testbed is controlled by a dual-processor PC. One processor runs a real-time system (RTX) and the other runs Windows XP. The real time system reads and writes to the I/O boards, reads the metrology data and runs control loop tasks, looping continuously at 5 kHz in synchronization with a precision external clock. Metrology data is provided by an FPGA-based signal processor which takes digital inputs from the metrology amplifiers and produces phase information up to 16 channels wide at 100 kHz. The real-time system's activity is controlled and monitored by active-X calls to shared memory. At the user level, the interface is via Matlab. At the basic level, one-line scripts implement active-X calls at the command line. These calls can be either typed at the console or combined into larger scripts or graphical user interfaces (GUIs) for ease of use. The overall system is adaptable, giving access to the lowest functions and data elements in the real-time system, and also providing high level functions such as the GUIs and near-real time graphing of sections of the signal streams. All data from the real time system can be logged to the hard disk continuously using a RAIDed set of high capacity drives. The data files are subsequently post-processed to select items of interest for further processing and display.

4. Nulling Experiments

4.1. Two-beam nulling

Deep two-beam nulls at near infra-red wavelengths had been achieved previously at JPL on a modified Mach-Zehnder[11] nuller. Null depths of one million, and as deep as two million when a polarizer was used, were obtained[9] using a CO_2 laser. That experiment was relatively small in size and drifted in alignment relatively slowly and therefore could be stabilized using a combination of dithering (modulation of the OPD to vary the null, coupled with a control loop that

determined the position of the deepest null), and manual alignment during the experiment. The larger Planet Detection Testbed however needed an improved approach. Since null stability is an important requirement for planet detection, the TPF-I flight design includes a laser alignment system for beam pointing and shearing control and the latest version of the PDT includes such controls (described below). However the original PDT had no such systems, and it was found that nulls of order 10,000 to 1 could be readily achieved, but deeper nulls were difficult to maintain owing to continuous alignment drift. Therefore means were devised to adjust and maintain alignment using the nulling detector signal as the feedback. The system relies on a two-dimensional dithering of a piezoelectrically controlled alignment mirror (a circular disturbance of the pointing) which imposes a signal of a certain phase on the null. Detection of this signal allows the control loop to correct the pointing so as to maintain the deepest possible null. With this system in place, nulls of 100,000 to one could readily be achieved.

4.2. Four-beam nulling and planet detection

Three different four-beam nulling experiments were performed, the first showing a four beam null of order 100,000 to one, the second showing faint planet detection by amplitude modulation of the planet source, and the third showing faint planet detection by phase modulation of the planet source. These experiments represent steps on the path to planet detection by phase modulation at the beam combiner, the subject of a forthcoming set of PDT tests. The presentation of results which follows below constitutes a review of progress in 2005. Further details of the experiments outlined here are given in references 12 and 13.

4.2.1. Four beam nulling

Accurate beam alignment is necessary to achieve similar beam intensities at the nulling detector. An initial manual alignment was done using an infrared camera to ensure that the beams appeared to be coaxial and co-linear at the cross-combiner beamsplitter. Following this alignment, each beam was individually aligned using a dither loop similar to that used to optimize the null, but in this case set up to maximize the intensity of each beam at the nulling detector. Between alignments, it was noticed that the beams tended to drift slightly which would, if not compensated for, limit the null depth.

The testbed is equipped with a set of optical delay lines allowing control of the optical path differences between the beams. Piezo-driven microstepping drives allow 10 mm of travel of a linear stage, with resolution down to ~30 nm. Also attached to this stage are piezoelectric linear actuators allowing 80 μm of travel. (The testbed also has a set of high speed, short travel actuators, which were not used in these tests.) These actuators were used to sweep through the fringe tracker fringe so as to locate the center of the white light fringe. In order to use the fringe trackers, the optical system was set up with a small amount of dispersion created by adding an extra thickness of ZnSe glass into one of each pair of beams. This allows the 10 μm fringe to be near null when the fringe tracker fringe is halfway between the peak and the trough, so that the null could be maintained using the fringe tracker. In these experiments however, it was easier to use the OPD dithering method to maintain the null, since alignment dithering was already required to maintain the nulls. The main use of the fringe trackers was therefore to allow a reproducible operating point to be set up on one particular laser fringe. This would also ensure that the relatively broadband planet fringe was constructively interfered. The cross-combiner phase could also be set up in the same way using the cross-combiner fringe tracker and metrology systems. The testbed layout for this experiment is schematically illustrated in figure 5.

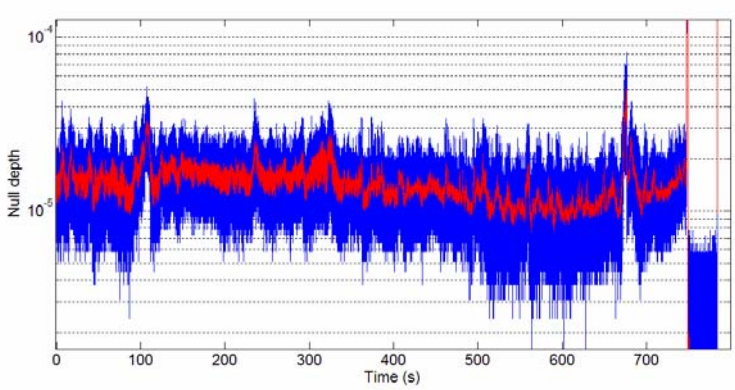

Figure 6: Nulling four infrared beams.

To null on four beams, four simultaneous dither loops were run at four different frequencies. Two loops run the OPD for the nullers, these dithers ran at 20 Hz and 30 Hz.

Two loops control the pointing on one of each pair of beams. These were run at 8 Hz and 12 Hz. The drifting of the uncontrolled beam of each pair was small, insufficient to significantly change the throughput which would have affected the measured null depth.

Figure 6 shows a plot of the null at the deepest section. The blue trace shows the spread in the apparent null depth caused largely by the imposed dithering. The red trace shows a smoothed version of the data, with a period of 0.1s. It can be seen that the null depth is approximately 250,000 to one during this section of the experiment. The data at the end shows the signal with all shutters closed, establishing a baseline. Calibrations of the null depth were performed at the end of the experiment (not shown here).

4.2.2. Planet detection by amplitude modulation

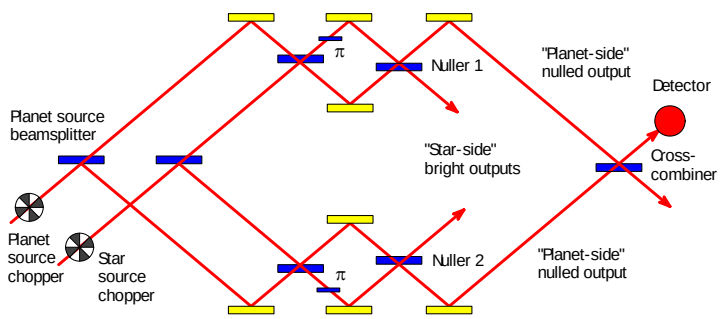

Figure 7: Layout of testbed for planet detection experiments.

The testbed layout for this experiment is schematically illustrated in figure 7. The four planet beams have been added, with the planet light chopper running at a different frequency to the star chopper. The difference was approximately 70 Hz. This frequency was chosen because it was not excited by the control loops and is therefore not normally seen in the output of the nulling detector. The planet signal intensity could be varied by changing the current to the thermal source, and cross-checked by shuttering off the star and making individual measurements of the four planet beam intensities. Three experiments were run, one with no planet, one with a faint planet, and one with a brighter planet. Figure 8 shows the results of these experiments in the form of spectra of the nulling signal. The planet signal appears as the spectral peaks at ~70 Hz. Because the difference frequency between the star and planet choppers varied somewhat, this data was processed as a spectral estimate by cutting the data record into one second long pieces, and the true planet signal amplitude was found by integrating the resulting spectral peak. The results of the integrations are shown as the two boxes. The upper box represents a contrast ratio of the planet compared to the star of 1 to 500,000, the other as a contrast ratio of 1 to 2,000,000.

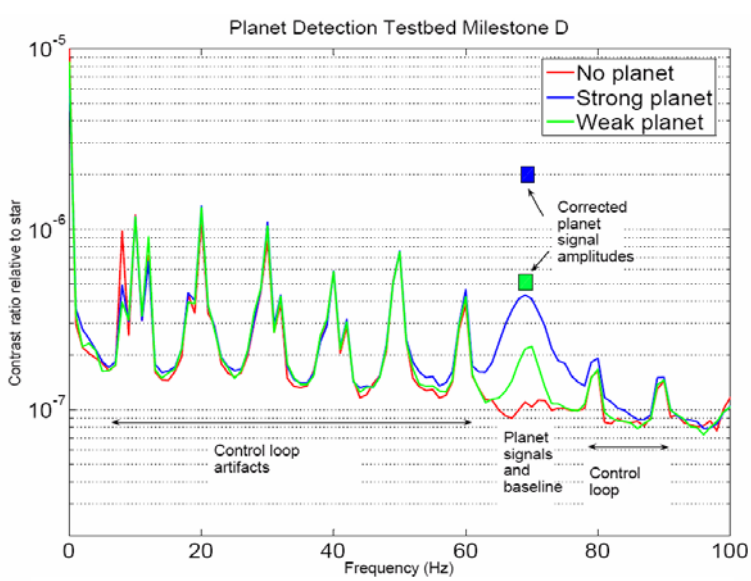

Figure 8: Frequency spectrum of the nulling detector output.

4.2.3. Planet detection by phase modulation

Closer to the TPF detection method, in this case the planet will be detected by causing it to move from one side of the star to the other. This is somewhat like making 180 degree stepwise rotations of the telescope array. Below, these two conditions will be referred to as chop states one and two. Referring again to figure 7 the planet source has been admitted with the planet light chopper now running synchronously with the star chopper, so that the star and planet beams are either both on or both off. The motion of the planet is produced by moving the planet source

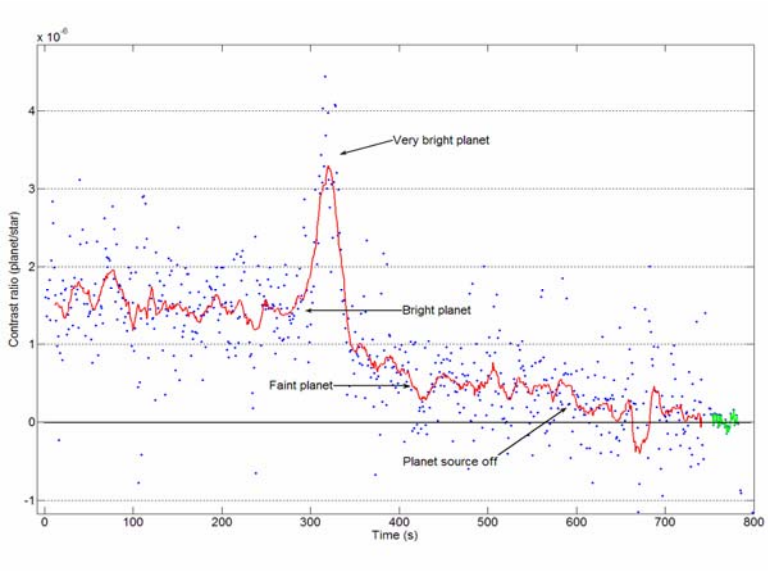

Figure 9: Planet detection using planet source phase chopping.

beamsplitter by plus and minus ¼ wave at 10.6 μm. Figure 9 shows the data from this experiment. The blue dots represent individual measurements at the null detector formed by differencing the light received while in chop state one from that received in chop state two and are similar to the data shown in figure 4 which shows the individual realizations of data in an unstable null. The red line on figure 9 is the raw data (which has a 1.1 s period) smoothed by calculating a rolling average 20 s long.

Initially the thermal source current was set at a moderate value, then raised for a short while and then reduced to a low value before being turned off. The null depth during this experiment was moderate at about 90,000. In the first part of the trace, the star to planet contrast ratio is ~600,000:1, and in the later part ~2,000,000:1.

5. Testbed development plans

The testbed has been rebuilt to enable phase chopping at the cross-combiner, thus simulating the TPF planet signal extraction plan. Also, a different method of planet light injection will be used, allowing the planet phase to be varied independently of the star, and enabling the planet to be positioned anywhere in the sky. This will enable simulation of formation rotations, and production of output data similar to that of figure 4. To incorporate this feature and also to provide better beam pointing control, the testbed has been rebuilt with an extension so that it forms a larger, T-shaped table. Also, changes have been made to the fringe tracking setup. Because the fringe tracker output is sensitive to beam tilting, the addition of the pointing stabilization system will also stabilize the fringe tracker. The fringe tracking detector optics have been altered to a fiber-coupled setup. Both single mode and multi-mode fibers can be accommodated and will be assessed for relative fringe tracker stability. The single mode fibers have performance advantages in terms of phase stability because of their reduced sensitivity to beam tilting, but will require much more accurate alignment with the science beam fiber.

6. Conclusion

In these experiments, the OPD and the alignment were maintained by the use of dithering techniques, which require a relatively strong source. So, these control techniques are unlikely to be useful for a space telescope. In the rebuild of the testbed, the controls will be based on an alignment laser system and a fringe tracking system, which will be architecturally similar to the envisaged flight control system. To reproduce space-like signal to noise ratios, will require further development.

These results demonstrate faint planet detections using nulling interferometry in a 4-beam beam combiner. Null depths up to 250,000:1 were achieved. Planet signals that are 2 million times fainter than the star were detected using two methods. These star:planet contrast ratios are close to the flight requirement of ~3 million to 1. New testbed developments are aimed at demonstrating this performance using optical path difference chopping in a flight-like beam combination method.

Acknowledgements

The authors would like to acknowledge the contributions of the other members of the testbed team: Hong Tang, Randall Bartos, Raymond Lam, Boris Lurie and Nasrat Raouf.

The work reported here was conducted at Jet Propulsion Laboratory, California Institute of Technology, under contract with NASA. Reference herein to any specific commercial product, process, or service by trade name, trademark, manufacturer, or otherwise, does not constitute or imply its endorsement by the United States Government or by the Jet Propulsion Laboratory, California Institute of Technology.

References

1. Biosignatures and Planetary Properties to be Investigated by the TPF Mission. D. J. Des Marais, M. Harwit, K. Jucks, J. F. Kasting, J. I. Lunine, D. Lin, S. Seager, J. Schneider, W. Traub, N. Woolf. JPL Publication 01-008, Rev. A, National Aeronautics and Space Administration, Jet Propulsion Laboratory, California Institute of Technology, Pasadena, California
2. Graded coronagraphic masks for high-contrast near-infrared imaging , Joseph C. Carson, Daniel W. Wilson, John T. Trauger Proc. SPIE Vol. 5905, p. 427-438, "Techniques and Instrumentation for Detection of Exoplanets II", Daniel R. Coulter; Ed. Aug 2005
3. Detecting nonsolar planets by spinning infrared interferometer, R. N. Bracewell. Nature 274, 780-781. 24 Aug 1978.
4. Deep nulling of laser light in a rotational shearing interferometer, S.R. Martin, E. Serabyn, G.J. Hardy. Proceedings of SPIE Volume: 4838. Interferometry for Optical Astronomy II. Ed. Wesley A. Traub. Feb 2003.
5. Array Configurations for a Space Infrared Nulling Interferometer Dedicated to the Search for Earthlike Extrasolar Planets , B. Mennesson, B. and J.M Mariotti, ICARUS 128, pp 202-212, 1997.
6. Systematic Errors in Nulling Interferometers, O.P. Lay, Applied Optics, vol. 43, pp. 6100-6123, 2004.
7. TPF Planet Detection Testbed: demonstrating deep, stable nulling and planet detection. Stefan Martin. IEEE Aerospace Conf. Big Sky, MT, 2005.
8. The flight instrument design for the Terrestrial Planet Finder Interferometer, S.R. Martin. Proc. SPIE Vol. 5905, p. 21-35, Techniques and Instrumentation for Detection of Exoplanets II; Daniel R. Coulter; Ed. Aug 2005
9. A Mid-Infrared Nuller for Terrestrial Planet Finder: Design, Progress and Results. Martin, S.R., Gappinger, R.O. , Loya, F.M., Mennesson, B.P., Crawford, S.L., Serabyn, E. Proc. SPIE 5170. Techniques and Instrumentation for Detection of Exoplanets. Ed. Daniel R. Coulter. Nov 2003
10. Testing Exo-planet Signal Extraction Using the Terrestrial Planet Finder Planet Detection Testbed. S.R. Martin, Piotr Szwaykowski, Frank Loya. "Techniques and Instrumentation For Detection Of Exoplanets II". Proceedings of SPIE Vol. #5905. August 2005.
11. Fully Symmetric Nulling Beam Combiners, Serabyn, E., Colavita, M.M. Applied Optics-OT, Vol. 40 Issue 10 Page 1668. April 2001.
12. Progress in four-beam nulling: results from the Terrestrial Planet Finder Planet Detection Testbed. S.R. Martin. IEEE Aerospace Conf. Big Sky, MT, 2006.
13. TPF-I Planet Detection Testbed: Progress in Testing Exo-planet Signal Detection. S.R. Martin, P. Szwaykowski and F.M. Loya. Direct Imaging of Exoplanets: Science and Techniques. Proceedings of the 200th Colloquium of the International Astronomical Union. Villefranche sur Mer, France, Oct 2005. Claude Aime and Farrokh Vakili Eds. Cambridge University Press.